

High-speed casting of metallic foils by the double-roller quenching technique

Y. V. MURTY

Cabot Corporation, Reading R & D, Box 1296, Reading, PA 19603, USA

R. P. I. ADLER

GTE Laboratories Incorporated, Waltham, MA 02254, USA

The ability to produce continuous metallic foils by double-roller quenching with a "mechanically-soft" system has been demonstrated. Significant process variables influencing foil dimensions and microstructures were determined for tin and Al-12 wt% Si foils. The foil formation process is controlled by both fluid and heat flow. The diameter of the circular jet used to supply liquid metal to the roller nip largely establishes the dimensions of useful products. A lower foil thickness processing limit of 0.015 cm is recommended for double-roller quenching based on operational considerations.

1. Introduction

The products from various rapid-quenching techniques come under the general classification of powder, flake, foil and wire. These products exhibit unique microstructures which may be amorphous, microcrystalline or have other structural refinements ideal for special engineering applications. These concepts spurred significant interest both in industrial and academic institutions in recent years, leading to the development of a number of processing techniques [1-8]. In addition, the favourable economics of producing near net-shape crystalline forms such as wire and foil directly from the melt would appear to justify using rapid-quenching technology by industry in many cases. Foil-like products (or ribbons) have been produced by melt extraction [3] and melt spinning [9] approaches where a single rotating substrate is used as a quenching medium.

The double-roller melt-spinning technique is still in the development state. It was originally used by Babic *et al.* [10] and Chen and Miller [11], to produce limited quantities of Al-Fe and Pd-Si alloy foils. The technique essentially consists of melting an alloy charge in a crucible and directing the liquid between a pair of rapidly counter-rotating rollers held together under pressure. This method was extended later to pro-

duce very small quantities of strips and flakes from a variety of metal alloys and refractory oxide mixtures [12-19]. An analytical model for the process has been developed recently by Miyazawa *et al.* [20].

Lewis *et al.* [15], from limited experiments, compared the microstructures produced by both double- and single-roller melt-spinning techniques. Foils produced by the double-roller technique, however, exhibited considerable deformation. Based on dendrite-arm spacing measurements as well as from an analytical estimate, they claimed an order of magnitude lower cooling rates (nominally 10^5 °C sec⁻¹) for the double-roller technique compared to the single-roller technique. While the accurate measurement of such high cooling rates is rather complicated, both of the methods are capable of producing refined microstructures. If the solidification of the strip is completed prior to exiting from the rollers, then the foil thickness is mainly governed by the heat-flow [21, 22]. This can only occur under certain experimental conditions, as will be clear later, particularly with the double-roller technique.

The aim of this investigation was to understand the foil-formation process so that continuous metallic foils could be made by the double-roller quenching technique. The solidification and mass-flow behaviour, as effected by various processing

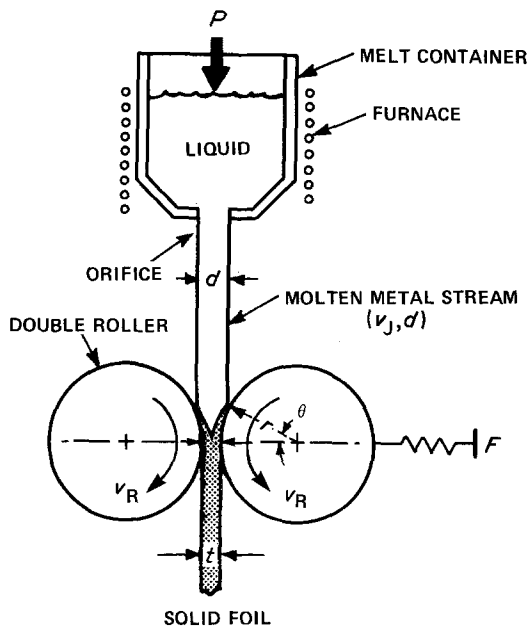


Figure 1 Conceptual representation of the double-roller quenching apparatus and operating parameters.

variables, are described and correlated with the quality and dimensions of the foil products.

2. Principles of operation

A schematic representation of the formation of strip by double-roller quenching is illustrated in Fig. 1. The typical solidification sequence is complex due to the interaction of both heat and mass transfer phenomena and, as such, cannot be described by any single mechanism. However, a general understanding of the sequence of events occurring during foil formation can be derived from the following two-dimensional model.

A liquid jet of diameter, d , contacts the cylindrical surface of the rollers rotating with speed, ω . Metal layers simultaneously solidify on each roll and converge together due to rotation and growth as they approach the nip section of the rollers. During this period, the remaining unsolidified liquid from the central pool is forced to spread laterally outward contributing to the final width of the foil, w . The resulting foil emerges from the nip and detaches from the rollers. The thickness of the primary solidified layer is a function of the contact time (or residence time) with the roller surface, while the overall thickness, t , of the foil is partially controlled by the roll-gap, g . The primary residence time, τ , is, in turn, governed by g and d . These functional parameters are related by the following equations:

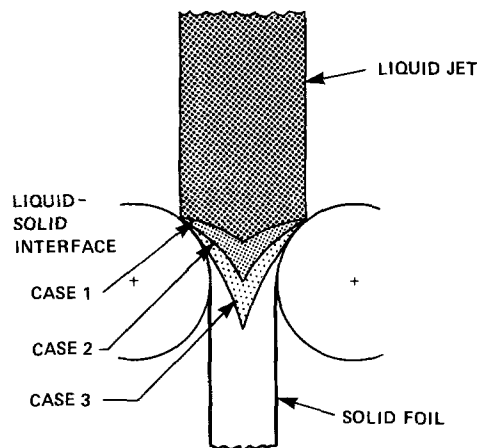


Figure 2 Illustration of the three classes of foil solidification during double-roller quenching.

$$\tau = \frac{60\theta}{2\pi\omega} \quad (1)$$

$$\theta = \cos^{-1} \left(1 - \frac{d-g}{2r} \right), \quad (2)$$

where θ is the foil-substrate contact angle in radians, r is the radius of the rollers and ω is the rotation-rate in revolutions min^{-1} .

The significance of individual parameters in Equations 1 and 2 on foil dimensions will be further discussed in the following sections.

The liquid mass flow-rate, Q , and jet velocity, v_j , is a function of the over-pressure, P , while the former is also proportional to the jet diameter, d . It is assumed that no break-up of the liquid jet occurs during its free travel. This was later confirmed experimentally from high-speed films of the jet profiles used in this investigation. The extent of outward lateral liquid flow during primary skin formation depends on the relative volumetric flow of the liquid entering into the nip section. For continuous foil formation, v_j and ω have to be coupled together in a proper ratio. The solidification prior to detachment is primarily controlled by conductive cooling into the rollers; after detachment the foil is cooled by radiative and convective exchanges with the environment.

Depending on the experimental conditions during double-roller quenching, there exist three general cases related to where the liquid-solid interfaces from the respective rollers merge to produce a completely solid foil. The three cases are shown schematically in Fig. 2.

In the first case, the liquid-solid interfaces

come in contact with each other prior to entering into the nip section forming a foil that is potentially thicker than the pre-set roll gap. Severe deformation of the foil should then be expected to occur in the nip section prior to the release of the foil from the rollers, a situation analogous to hot rolling. However, whenever the roll constraint force, F , is not great enough to produce complete mechanical deformation of the solid strip, the final thickness of the foil will be greater than the pre-set roll gap. Conditions for this mode of solidification are favoured when relatively large diameter orifices (compared to the roll-gap dimensions) are employed at lower mass flow and roller rotation rates.

In the second case, the liquid–solid interfaces from both the rollers join right in the nip forming the final thickness of the foil with or without slight accommodation of the effective gap spacing.

In the third case, the foil completes solidification below the nip section. At the nip section, the primary solidified layers should be thick enough to contain the remaining liquid within the cross-section of the foil if a continuous foil is to be formed. The final dimensions of this foil are then established while this partially-solidified strip goes through the roll gap. The remnant liquid contained within the foil will solidify more slowly by heat removal through convection and radiation.

The foil thickness in the last two cases is expected to be close to the pre-set roll gap.

3. Experimental procedure

The experimental set-up capable of processing continuous metallic foils is shown in Fig. 3. The double-roller quenching apparatus consists essentially of two internally water-cooled copper rollers. These 15 cm diameter rollers are driven by a variable speed d.c. motor with a single belt-drive to synchronize the rotation speeds of both rollers up to $2700 \text{ rev min}^{-1}$. One roller is mounted with a fixed central axis of rotation while the other one is spring-loaded and can be horizontally translated providing any arbitrary relative positioning. Thus, it is possible to adjust the restraint force between the rollers as well as their nip spacing. In addition, the spring-loading feature acts as a safety measure, allowing roller separation whenever excess metal build-up in the nip might otherwise destroy the roller surface.

The melt delivery assembly consists mainly of

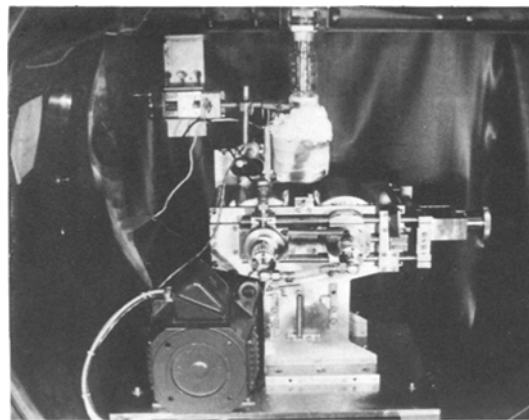


Figure 3 Overall view of double-roller quenching assembly.

a quartz pressure vessel located inside a resistance heating coil. This assembly is mounted on a movable stage so that the positioning of the crucible relative to the roller-quenching assembly can be performed either prior to or during the experimental run. The metal charge of several hundred grams is melted in the quartz vessel using resistance heating with an argon blanket to prevent oxidation. After the charge is molten, generally with a super-heat of about 50 to 100°C , the argon over-pressure is increased to a specified value causing the liquid metal to be forced through a circular orifice at the base of the vessel forming a jet which passes into the nip of the rollers. At pressures of 1.4×10^2 to $6.9 \times 10^2 \text{ Nm}^{-2}$, a stable jet forms with a relatively constant mass flow rate, because the head-height pressure can be neglected. In order to obtain reproducible results, it was necessary carefully to align the liquid jet with the centre of the roll gap. The quenched foil is collected below the quenching assembly after completion of the run. The best foil release condition occurred when the liquid jet was directed properly into the nip.

The process variables examined in this investigation were the velocity, restraint force, and pre-set gap of the roller-quenching assembly and the velocity and mass flow-rate of the liquid jet. The effect of these variables, both individually and in various combinations, on the foil quality was evaluated. Both tin and a binary Al–12 wt% Si alloy were selected as the materials for this investigation. The binary aluminum alloy was prepared from commercial purity virgin materials using standard melting procedures. The Al–12 wt% Si alloy was helpful in understanding the solidifi-

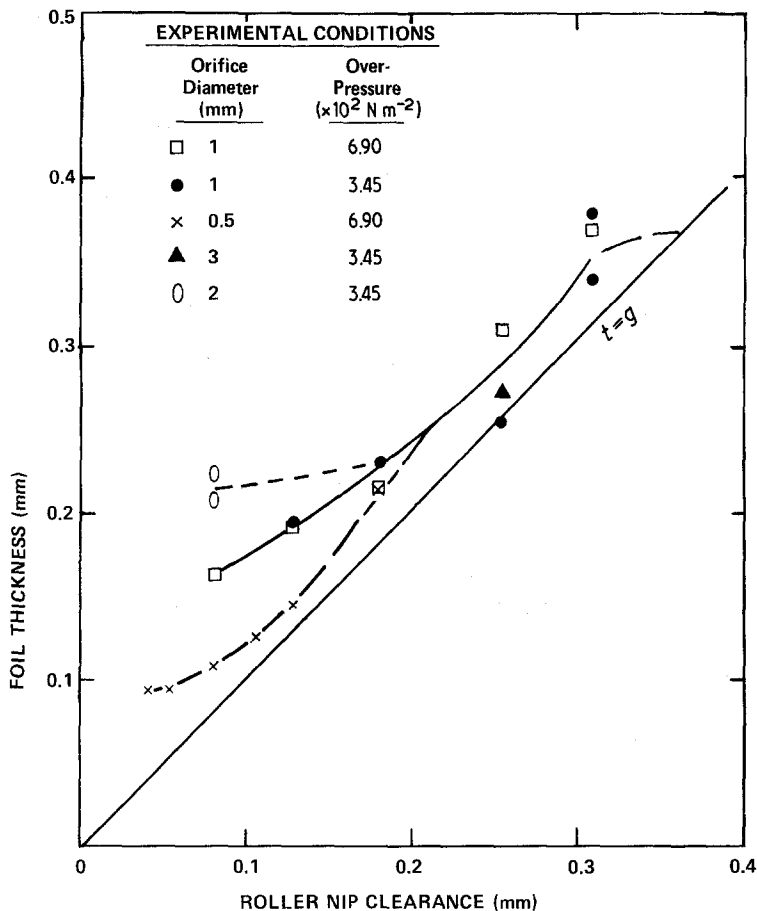


Figure 4 Variation of tin-foil thickness with processing parameters with 1 mm diameter melt delivery orifice.

cation behaviour through interpretation of the microstructure.

4. Results and discussion

4.1. Dependence of foil thickness on process variables

The response of foil thickness to several process parameters under some experimental conditions is shown in Figs 4 and 5 for tin. Continuous foils are produced when the ratio of jet velocity, v_J , to the roller velocity, v_R , was kept between 0.5 and 1.0, see Fig. 4. Within this useful working regime, the foil thickness was relatively insensitive to the relative velocity, v_J/v_R . For cases where the jet velocity is greater than the roller velocity, the accumulation of liquid metal occurring inside the roll nip complicates the lateral flow pattern of the solidifying liquid metal. Consequently these foils exhibit gross thickness variations with the bars representing the high and low values of thickness. For conditions where the jet velocity is substantially less than the roller velocity, that is, where $v_J/v_R \leq 0.5$, the supply of liquid is insuf-

ficient and a periodically discontinuous foil results. The smoothly tapered ends of such discontinuous foils could be clearly distinguished from continuous ribbons with broken ends caused by the impact after leaving the roller nip. Thus, a continuous balance between the incoming jet velocity and the roller velocity is essential for the production of uniform cross-sectional continuous foil.

Although the foil thickness is relatively independent of relative velocity within the useful working regime ($0.5 \geq v_J/v_R \leq 1.0$), it responds very well to initial roll gap, g (see Fig. 5). Also indicated, is the relationship corresponding to $t = g$. The experimentally-measured foil thickness in Fig. 5 was always greater than roll gap, except for few experimental conditions. This indicates that the solidification of the foil is completed prior to the nip leading to thickness greater than g . Increase in roll-gap spacing, with a given jet diameter, nearly increases the foil thickness and moves the intersection point where the two liquid-solid interfaces meet from above the nip

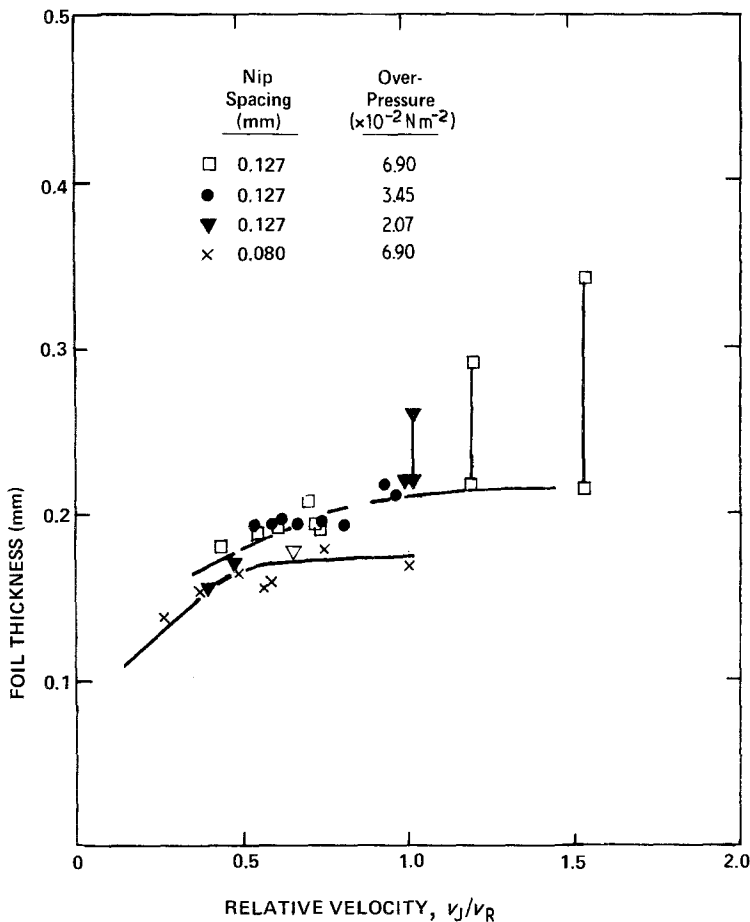


Figure 5 Primary relationship between tin-foil thickness and roller-nip spacing at constant roller velocity, $v_R = 480 \text{ cm sec}^{-1} \geq 1.5 v_j$.

section to below the nip section (sequentially from Case 1 to 2 and to 3, as shown in Fig. 2). This trend can be more clearly evidenced from the data shown in Tables I and II for Sn as well as for Al-12 wt% Si alloy. For substantially larger g values the thickness of the solidified "skin" is insufficient to contain the remainder of the liquid so that it effectively pours right through without forming a foil. For example, foil formation did not occur with 1.0 mm diameter tin-jet when the roller spacing was kept greater than 0.3 mm. Thus, within the practical limits, it can be seen that the foil thickness is mainly governed by the roller gap, g , with secondary dependence on the relative velocity and jet diameter.

Both increase in roller spacing at constant jet diameter and decrease in jet diameter at constant roller spacing will reduce the contact length between the solidifying foil and the roller surface over which the conductive heat transfer operates. Foil solidification is predominantly dominated by this conductive heat-flow. Reduction in contact length, if all other conditions were kept constant,

should reduce the solidification time and, hence, the foil thickness, if the foil formation is controlled by conductive heat transfer alone. Obviously, the experimental trends shown for tin in Fig. 5, clearly point to this not being the case. Although the foil thickness responded well to the jet diameter at lower g values, its response was not so predominant at higher g values. Furthermore, the foil thickness increased even with

TABLE I Effect of roll gap and residence time on foil thickness for Al-12 wt% Si alloy

Orifice diameter (cm)	Residence time (sec)	Roll gap (cm)	Foil thickness (cm)
0.075	0.001 49	0.0076	0.015
0.1	0.001 50	0.0076	0.015
0.15	0.002 16	0.0076	0.023
0.2	0.002 17	0.0076	0.019
0.15	0.002 65	0.02	0.032
0.2	0.002 07	0.025	0.023
0.2	0.001 99	0.038	0.030
0.3	0.002 53	0.038	0.035
0.45	0.002 78	0.038	0.042

TABLE II Dependence of foil dimensions on various process parameters

Material	Surface velocity (cm sec ⁻¹)	Roll gap (cm)	Orifice diameter (cm)	Over-pressure ($\times 10^2$ N m ⁻²)	Flow rate (g cm ⁻¹)	Foil thickness (cm)	Foil width (cm)
Sn	480	0.013	0.1	2.07	15.0	0.02	0.30
Sn	480	0.013	0.1	3.45	18.0	0.02	0.35
Sn	480	0.013	0.1	6.90	25.0	0.02	0.40
Sn	560	0.0076	0.2	3.45	73.0	0.02	1.04
Sn	560	0.0076	0.2	6.90	100.0	0.021	1.75
Sn	560	0.038	0.3	3.45	163.0	0.035	1.1
Sn	438	0.038	0.3	6.90	225.0	0.033	2.13
Al-12 wt% Si	480	0.0076	0.15	6.90	34.0	0.023	1.16
Al-12 wt% Si	638	0.038	0.3	2.07	77.0	0.038	1.18
Al-12 wt% Si	398	0.038	0.3	3.45	97.0	0.03	2.1
Al-12 wt% Si	638	0.038	0.3	6.90	137.0	0.03	1.63

increase in roller spacing, which had been expected to decrease the contact distance. Thus, the foil formation during double-roller foil casting is governed by both heat flow and fluid flow. Any theoretical models dealing with this process should consider the combined effects of these phenomena. The correlation between the experimental values obtained herein and the analytical predictions [20] is currently under investigation [23].

4.2. Dependence of foil width on process variables

The variation of foil width with relative velocity, v_J/v_R , for tin foils made with 1 mm diameter orifices is illustrated in Fig. 6. The jet mass flow-rate becomes more important in establishing the final width of the foil, as shown in Table II. When smaller nip spacings are employed, the liquid must spread laterally through relatively greater distances

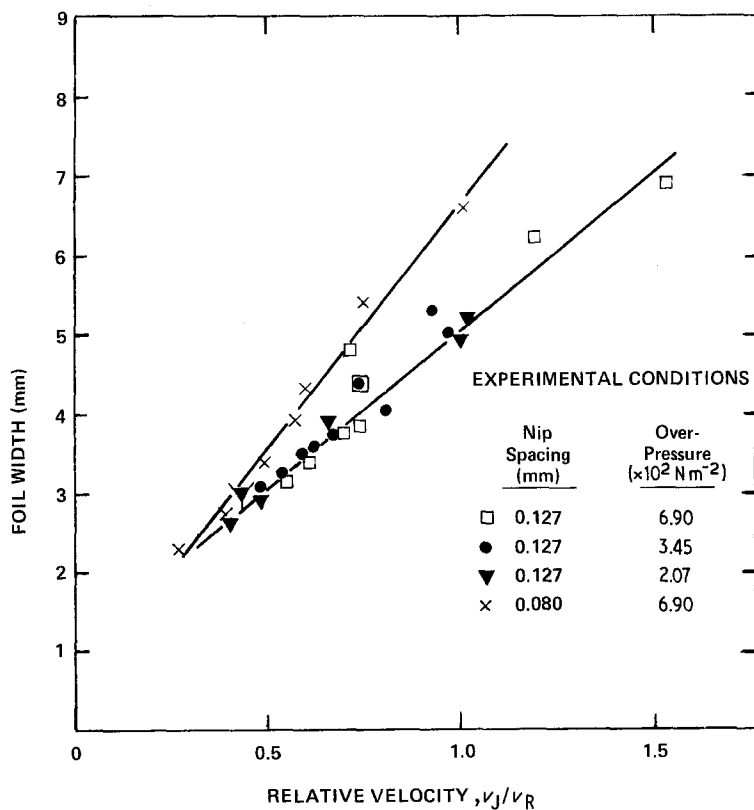


Figure 6 Variation of tin-foil width with processing parameters with 1 mm diameter melt delivery orifice.

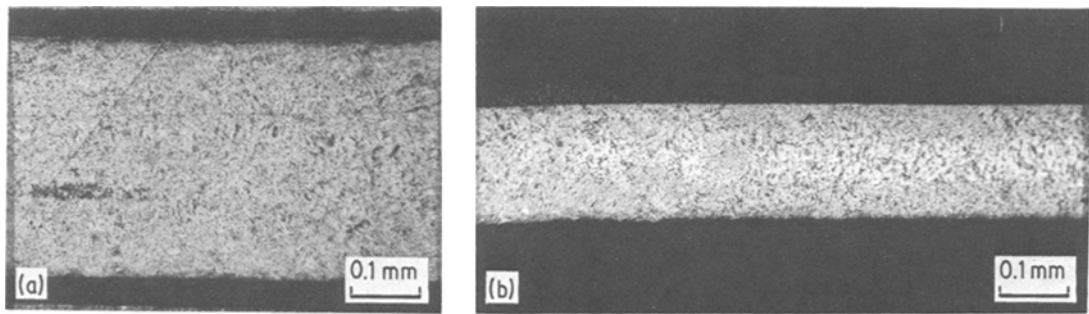


Figure 7 Microstructures of rapidly solidified Al-12 wt% Si processed to include (a) light or (b) heavier thickness accommodations. (a) $g = 0.18$ mm, $t \approx 1.5$ g. (b) $g = 0.08$ mm, $t \approx 2.5$ g.

perpendicular to the axis of foil movement. While this occurs, the liquid also loses heat to the rollers; thus, the related increase in viscosity can cause non-uniform spreading. This in turn produced foils with rough edges having a cyclic pattern. Hence, it is apparent that unlimited-width foils cannot be made by arbitrarily increasing orifice diameter and jet velocity. On the other hand, by careful adjustment of the mass flow-rate (including the v_j/v_R ratio) and the roll gap, the formation of continuous, dimensionally uniform foils can be attained.

4.3. Structure of as-cast foil

Metallographic evaluation of the as-cast foils for the Al-12 wt% Si alloy provided a useful insight into the foil-formation process. A common microstructural feature for these transverse cross-sections (Figs 7 and 8) is the existence of a primary solidification zone with highly refined grains; these rapidly-solidified chill zones grow from both contact surfaces and extend to varying degrees into the centre of the foil. The extent of this chill zone depends on the initial conditions of foil solidification. The chill-zone microstructure was so fine that no quantitative measurements of dendrite-arm spacing and, hence, an indication of the cooling rate, could be made even from high magnification optical micrographs.

Under certain processing conditions, shown in Figs 7a and 8a, the chill zone fills the entire foil cross-section. When relatively small roll gaps (0.18 mm) are combined with larger orifice diameters (1.5 mm), the resulting foil thickness, t , is greater than the initial pre-set gap distance, g ; a clear indication that the foil has been completely solidified prior to entering the nip. The calculated residence time using Equation 1 is approximately

0.0023 sec for this processing condition. Assuming a 700°C melt temperature and a 300°C foil release temperature, the corresponding upper limit for the cooling rate would be $1.7 \times 10^6\text{C sec}^{-1}$. This qualitative cooling rate prediction is consistent with values reported for other rapid-quenching techniques [9, 19, 20].

Under different processing conditions, with a substantially smaller gap (0.076 mm) and a larger jet diameter (2.0 mm) a duplex microstructure forms. This structure consists of a narrow chill zone at each contact surface and a coarser structure in the central core (see Fig. 7b). Even though the calculated residence time was only slightly shorter (0.0021 sec), a different coupling mix between heat and mass flow has occurred in these two cases. These two distinct zones have non-equilibrium eutectic particles (coarse) whose dimensions are clearly different. Previously reported [24, 25] duplex microstructures for splat-cooled Al-4.5 wt% Cu and Fe-25 wt% Ni alloys were attributed to the transition from columnar to equiaxed grain growth during solidification. The microstructural features of Figs 7b and 8d suggest a similar transition in the solidification mechanism. This transition occurs, according to one conventional solidification theory [26], when fluid flow forces knock the tips off the columnar dendrites, and these dendrite fragments subsequently act as random growth sites in the remainder of the liquid. For certain double-roller foil-forming conditions, the specific combination of turbulent fluid flow and rapidly dropping temperature in the remaining liquid core of the foil could result in a similar transitional phenomena. The presence of rounded islands (which have very fine micro-features) in the central section of Fig. 7b and the irregular zone

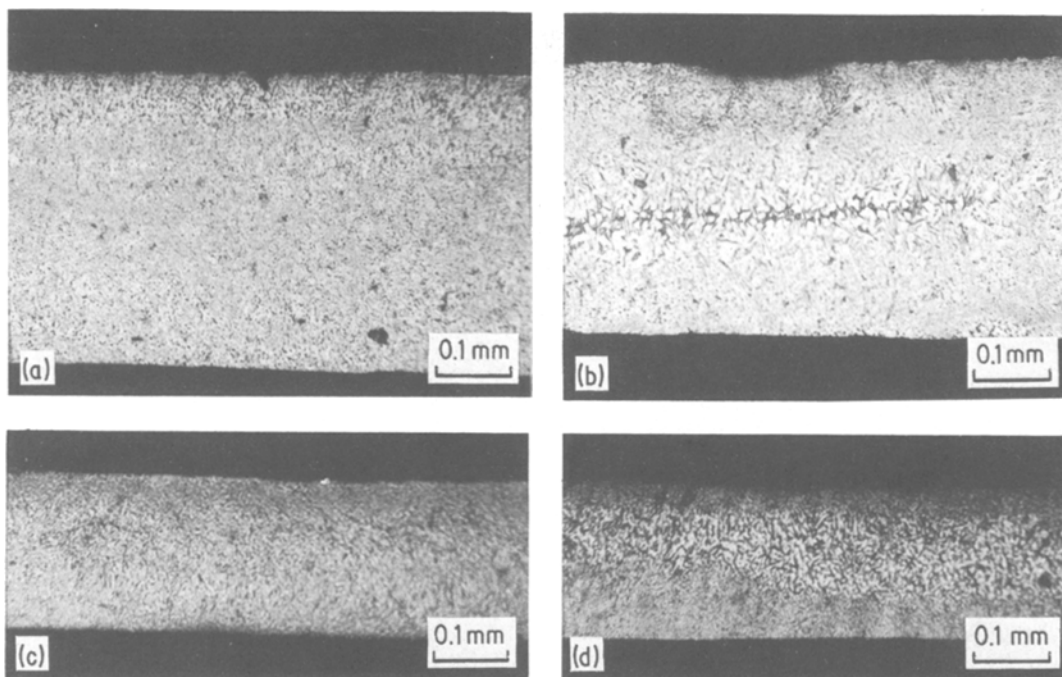


Figure 8 Microstructures of rapidly-solidified Al–12 wt% Si foils processed to have minimal thickness accommodation. Foil cross-sections of (a) central (one-zone) and (b) near-edge (double zone and remnant fluid) regions from a foil made using a 3 mm diameter jet and similar (c) central (one zone) and (d) near-edge (double zone) regions from a foil made using a 2 mm diameter jet.

boundary of Fig. 8b corroborate this concept of two-phase turbulent flow.

Foil thicknesses close to the preset roll gap can be attained for properly matched jet–substrate parameters even with large amounts of fluid rearrangement. The microstructures for two such conditions are shown in Fig. 8. For both cases, the longitudinal mid-section of the foil consists only of the chill zone; the corresponding longitudinal edge regions have a duplex microstructure. This dual microstructure results from extensive lateral flow of the liquid formerly in the core. Note that the liquid mass flow-rate for the 3 mm diameter jet was nearly double that for the mass flow-rate for the 2 mm diameter jet. Thus, the presence of a pronounced central vein (a resultant of a remnant liquid that solidified more slowly after foil detachment from the rollers) is a reasonable feature in Fig. 8b. This solidification microstructure is consistent with Case 3 type solidification (Fig. 2). Under extreme Case 3 conditions, where a considerable volume of liquid is present, the product tends to separate into two sheets where each half tracks with its respective quench substrate.

4.4. Double-roller foil-quenching process limitations

Production of Sn and Al–12 wt% Si alloy foils between 0.015 to 0.040 cm in thickness was achieved in this investigation. Tables I and II show the foil dimensions along with other appropriate processing conditions. Processing of foils thinner than 0.015 cm will require smaller jet-forming orifice diameters and extremely low roll-gap clearances. Under these conditions, severe deformation to the foils and associated loss of mechanical properties due to surface-related defects have been reported [15]. To produce such significant amounts of deformation, hard low-conducting roller materials were required to prevent roller surface damage under the high processing forces used. For the present investigation, the production of thicker foils (> 0.015 cm) was examined with higher conductivity copper rollers. Most of the double-roller quenching experiments were conducted at a roller constraint force of 91 kg. The utility of this relatively “soft” system to produce foils combined with the safety feature of spring-loading to keep roller damage to a minimum is a significant processing demonstration.

When the roller constraint force was reduced to 45.5 kg the resulting foils did not exhibit drastic differences in dimensions. The foils were slightly thicker with an associated minor reduction in width.

To take full advantage of rapid solidification by double-roller quenching, the extent of deformation to the foil should be minimized and a highly conductive substrate such as copper should be employed. Although the solidifying foil can take a small amount of deformation in the mushy liquid–solid region, the amount of deformation should be controlled during the process. It is expected that any significant deformation to the hot solid product very close to its melting point would damage the foil by creating defects such as hot cracks that are inherent to hot-rolling practice. This problem might become severe when working with brittle crystalline materials that are otherwise particularly suited to rapid solidification processing. With this empirical insight, efficient production of very thin foils (< 0.015 cm) would be better accomplished using the single-roller melt-spinning technique.

5. Conclusions

(a) The overall phenomena of foil formation by double-roller quenching involves a combination of heat and mass flow factors within an operational window of processing parameters. At one processing limit, a minimal amount of fluid rearrangement of the cylindrical jet shape is required to occur in order to allow sufficient heat transfer to permit solidifications; in this region of the processing window, heat flow is the dominant mechanism. As the degree of fluid rearrangement increases, the system approaches the other side of the processing window where mass flow is the dominant mechanism.

(b) The primary processing parameters that control foil dimensions and continuity are the relative jet velocity, v_J/v_R , the jet-mass flow-rate and the roller-gap spacing.

(c) The recommended dimensional regime for roller-quenching continuous foils is for thicknesses greater than 0.015 cm. For thinner foils, operational limitations become more severe and alternative approaches such as single-roller melt-spinning would be more advisable.

(d) The use of moderate roller restraint forces, applied through spring-loading, provides a “mechanically-soft” double-roller quenching system. This

relaxation feature permits the system to adapt itself to a dynamically stable operating configuration. Thus, for most combinations of operating parameters, this system rapidly adjusts to a steady-state condition capable of the long-term production of foils with reproducible dimensions.

(e) Operating criteria necessary for producing dimensionally-uniform foils were identified: (i) for foil continuity the relative velocity ratio, v_J/v_R , should be between 0.5 and 1.0; (ii) for constant-width foils with minimal edge finish variations excessive spreading of the liquid jet diameter should be minimized; and (iii) the best ranges for producing foils with uniform thickness are defined by phenomenological limits where the upper limit is due to the heat-transfer constraints where incomplete solidification results in the formation of a useless product and the lower limit occurs because the system becomes mass-transfer limited where dimensional uniformity is difficult to maintain.

(f) the diameter of the circular jet is a critical parameter governing to a great extent the nominal width and thickness dimensions of the resultant foil product.

Acknowledgements

The authors would like to thank Dr D. M. Koffman for helpful discussions and guidance during the course of this investigation. The twin-roller equipment was creatively designed by Messrs A. Woronicki and T. J. Gorsuch. The contribution of Mr W. C. Allen in de-bugging and then operating this system (including the taking of experimental measurements) for this study is greatly appreciated.

References

1. J. J. GILMAN, *Metal Prog.* **118** (1979) 42.
2. S. R. ROBERTSON, T. J. GORSUCH and R. P. I. ADLER, in Proceedings of the International Conference on Rapid Solidification, Reston, November, 1977, edited by R. Mehrabian, B. H. Kear and M. Cohen (Claitor Publishing, Baton Rouge, LA, 1978) p. 188.
3. R. E. MARINGER and C. E. MOBLEY, *Wire J.* **12** (1979) 70.
4. M. R. GLICKSTEIN, R. J. PATTERSON and N. E. SHOCKEY, in Proceedings of the International Conference on Rapid Solidification, Reston, November 1977, edited by R. Mehrabian, B. H. Kear and M. Cohen (Claitor Publishing, Baton Rouge, LA, 1978) p. 46.
5. N. J. GRANT, in Proceedings of the International Conference on Rapid Solidification, Reston, November, 1977, edited by R. Mehrabian, B. K. Kear

- and M. Cohen (Claitor Publishing, Baton Rouge, LA, 1978) p. 230.
6. P. G. BOSWELL and G. A. CHADWICK, *J. Phys. E.* **11** (1976) 523.
 7. S. A. MILLER and R. J. MURPHY, *Scripta Met.* **13** (1979) 673.
 8. J. P. PATTERSON and D. R. H. JONES, *Metals Technol.* **8** (1981) 103.
 9. J. H. VINCENT, H. A. DAVIS, J. G. HERBERTSON, in Proceedings of the Symposium on the Continuous Casting of Small Cross-Sections, TMS-AIME Fall Meetings, Pittsburg, Pennsylvania, October, 1980, edited by Y. V. Murty and F. R. Mollard (AIME, Pennsylvania, 1980).
 10. E. BABIC, E. GIRT, R. KRESNIK and B. LEONTIC, *J. Phys.* **3** (1970) 1014.
 11. H. S. CHEN and C. E. MILLER, *Rev. Sci. Instrum.* **41** (1970) 1237.
 12. J-P. H. A. DURAND, MSc Thesis, MIT (1972).
 13. T. SUZUKI and A. ANTHONY, *Mater. Res. Bull.* **9** (1974) 745.
 14. J. BEDELL, U.S. Patent Number 3 863 658.
 15. B. G. LEWIS, I. W. DONALD and H. A. DAVIES, in Proceedings of the Sheffield International Conference on Solidification and Casting, July 1977 (The Metals Society, London, 1979) p. 490.
 16. E. GIRT *et al.* *Fizika* **9** (1977) 19.
 17. B. LEONTIC, J. LUKATELA, E. BABIC and M. OCKO, "Practices of Rapidly Quenched Metals III", **3** (The Metals Society, London, 1978) p. 41.
 18. V. V. BARSUKOY, P. G. KALASHNIKOV, G. C. CAREV, G. A. IAROVINSKI and D. I. IASSKII, *Liteinoe Proizvod* **232** (1978) 22.
 19. A. R. E. SINGER, A. D. ROCHE and L. DAY, *Powder Met.* **23** (1980) 81.
 20. I. M. MIYAZAWA and J. SZEKELY, *Met. Trans.* **12A** (1981) 1047.
 21. H. JONES, in Proceedings of the International Conference on Rapid Solidification, Reston, November 1977, p. 28.
 22. G. R. ARMSTRONG and H. JONES, Proceedings of the Sheffield International Conference on Solidification and Casting, July 1977, (The Metals Society, London, 1979) p. 454.
 23. I. M. MIYAZAWA, Y. V. MURTY, R. P. I. ADLER and J. SZEKELY, to be published.
 24. T. Z. KATTAMIS, W. F. BROWER and R. MEHRABIAN, *J. Crystal Growth* **19** (1973) 229.
 25. T. Z. KATTAMIS, Y. V. MURTY and J. A. REFNER, *ibid.* **19** (1973) 237.
 26. G. W. COLE and G. F. BOLLING, *Trans. Met. Soc. AIME* **245** (1969) 725.

*Received 4 February
and accepted 10 November 1981*